

## Contrast in transmission spectroscopy of a single quantum dot

B. D. Gerardot,<sup>a)</sup> S. Seidl, P. A. Dalgarno, and R. J. Warburton  
*School of Engineering and Physical Sciences, Heriot-Watt University, Edinburgh, EH14 4AS,  
 United Kingdom*

M. Kroner and K. Karrai  
*Center for NanoScience, LMU, Geschwister-Scholl-Platz 1, 80539 Munich, Germany*

A. Badolato and P. M. Petroff  
*Materials Department, University of California, Santa Barbara, California 93106*

(Received 25 January 2007; accepted 4 May 2007; published online 30 May 2007)

The authors perform transmission spectroscopy on single quantum dots and examine the effects of a resident carrier's spin, the incident laser spot size, polarization, and power on the experimental contrast. They demonstrate a factor of 5 improvement in the maximum contrast by using a solid immersion lens to decrease the spot area. This increase yields a maximum signal to noise ratio of  $\sim 2000 \text{ Hz}^{-1/2}$ , which will allow for megahertz detection frequencies. The authors anticipate that this improvement will allow further investigation of spectral fluctuation and open up the feasibility for an all-optical readout of an electron spin in a quantum dot. © 2007 American Institute of Physics. [DOI: 10.1063/1.2743750]

The ability to process quantum information requires access to a highly coherent two-level system.<sup>1</sup> Zero-dimensional semiconductor quantum dots (QDs) are an attractive solid-state host for such systems due to their reduced spin relaxation<sup>2</sup> and decoherence mechanisms compared to bulk or quantum wells. An optically driven exciton<sup>3</sup> and the spin state of a single carrier<sup>1</sup> in a QD are two such candidates. Photoluminescence (PL) spectroscopy is commonly used to characterize optically active QDs. In this method, carriers generated above the ground state of the QD relax to the lowest energy excited state through a generally incoherent process. While this technique is useful for probing the energy levels, charged states, and fine structure of a QD, the relaxation process and the presence of other carriers in excited states introduce decoherence.

A complementary experimental approach to PL is laser spectroscopy, in which the differential transmission of a single QD as a function of laser detuning is measured.<sup>4-7</sup> Laser spectroscopy provides two significant advantages over PL: sub- $\mu\text{eV}$  resolution and the well-defined preparation of states in a QD. The high-resolution provides access to the true line shape and linewidth of the transition. Investigation of the line shape can indicate interference effects,<sup>8,9</sup> whereas deviations from the ideal homogeneous linewidth can be caused by a nonradiative processes such as tunneling<sup>7</sup> or spectral fluctuations due to environmental effects.<sup>6</sup> The well-defined preparation of states in transmission spectroscopy is a result of good optical selection rules in the QD owing to the inherent lattice symmetry. Resonant excitation of a transition will transfer the polarization of the incident laser light to the exciton, allowing preparation of the individual electron and hole spins. This capability permits the optical initialization<sup>10</sup> and readout<sup>11</sup> of an electron spin.

The maximum change in transmission (i.e., the contrast) is a measure of the ratio of light resonantly scattered by the dot compared to the incident laser intensity. However, detecting the resonantly scattered laser light from a self-assembled

QD is a nontrivial experiment. Here we explore how the polarization, power, and spot size of the incident laser all affect the contrast. With a hemispherical solid immersion lens (SIL) we achieve a spatial resolution of  $\sim 350 \text{ nm}$  full width at half maximum (FWHM) for 950 nm wavelength ( $\lambda$ ) light. This increased resolution yields an increase in the experimental contrast by a factor of 4.8, and a maximum contrast of  $\sim 6\%$  is observed in our system. We also demonstrate that the spin state of a resident electron in the QD contributes to the ultimate contrast. Current measurements use integration times of 0.1–1.0 s, but motivated by the exciting possibility to directly observe spectral fluctuations or carrier spin flips, we consider the suitability for microsecond measurement times in transmission spectroscopy of a single QD.

We use a confocal microscope with diffraction-limited resolution to perform both PL and transmission spectroscopies. The system's spatial resolution was determined by measuring the differential transmission of a focused laser spot as it traversed a metal/glass interface [Fig. 1(a)]. The FWHM of the spot diameter ( $\Delta x$ ) without (with) a SIL was measured to be  $755 \pm 10$  ( $344 \pm 3$ ) nm for  $\lambda = 950 \text{ nm}$ . For a focused plane wave,  $\Delta x = (0.52\lambda) / (\text{NA}_{\text{obj}} n)$ , where  $\text{NA}_{\text{obj}}$  is the numerical aperture of the objective lens and  $n$  is the refractive index of the material. For  $\lambda = 950 \text{ nm}$ ,  $\text{NA}_{\text{obj}} = 0.65$  and  $n = 1.0$  (air);  $\Delta x$  is 760 nm. Using a high-index glass ( $n = 2.0$  for  $\lambda = 950 \text{ nm}$ ) hemispherical SIL directly on top of the semiconductor sample surface yields  $\Delta x = 380 \text{ nm}$ . This experiment demonstrates diffraction-limited performance for our system and we measure that using a glass SIL reduces the spot area by 4.8x.

Our sample grown by molecular beam epitaxy consists of InGaAs QDs embedded in a metal insulator semiconductor field-effect transistor device which allows control of the QD charge state.<sup>6</sup> The QDs are located 136 nm below the GaAs-vacuum interface to ensure that the resonance line shape is absorptive [determined by  $\lambda / (2n)$ ] rather than dispersive.<sup>9</sup> The QD energy is modulated via Stark shift and a lock-in amplifier is used to measure the differential transmission. A Si *p-i-n* detector (Thorlabs FDS 100) is mounted

<sup>a)</sup>Electronic mail: b.d.gerardot@hw.ac.uk

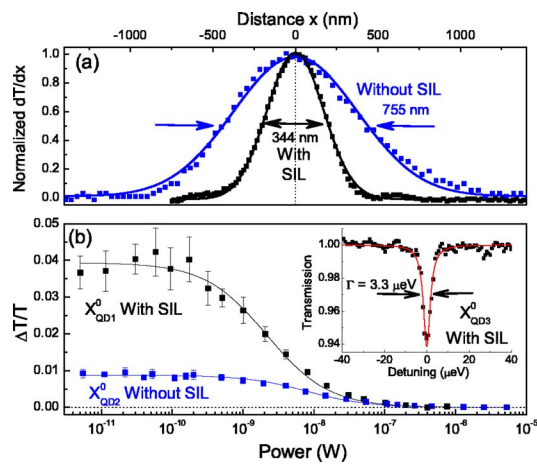


FIG. 1. (Color online) (a) Differential transmission as a laser spot traverses a metal/glass interface (solid lines are Gaussian fits to the data). (b) Saturation curves for two different  $X^0$  transitions with and without the use of a SIL. In the low power regime a SIL improves the contrast by  $4.48 \pm 0.41$  times for these particular QDs. At higher powers the curves converge due to the saturation as expected for a two-level system (solid lines). The inset shows the transmission of a different  $X^0$  transition as a function of detuning. Here, the contrast is 6.02% and the measured linewidth is  $3.3 \mu\text{eV}$ .

directly below the sample at 4 K inside the cryostat and a current amplifier (Femto DLPCA-200) is positioned near the cryostat to amplify the signal sent to the lock-in amplifier.

Figure 1(b) shows typical results for the contrast of a neutral exciton ( $X^0$ ) on and off the SIL in two different QDs. The measurement, over six decades in power, is made using linearly polarized light to maximize the contrast (see inset in Fig. 2). Due to the electron-hole exchange interaction, the bright exciton lines are nondegenerate and linearly polarized.<sup>12</sup> We have characterized the contrast of  $\sim 30$  different QDs. The statistics on all QDs measured show contrast in the low power regime of  $3.7 \pm 0.7\%$  ( $0.77 \pm 0.3\%$ ) with (without) a SIL, demonstrating that the contrast is improved by a factor of  $4.8 \pm 2.1$  due to the reduction in spot size. The vacuum level/first excited state transition of a QD behaves like a two-level system due to its atomlike character. Therefore, absorption of the transition saturates in the limit of a strong driving field resulting in a decreased contrast and increased linewidth on resonance.

The inset of Fig. 1(b) shows the transmission of an  $X^0$  in a different QD with 6% contrast, the largest contrast we have observed to date. The measured linewidth  $\Gamma$  for this transition is  $3.3 \mu\text{eV}$ . Using time-resolved PL, we have directly

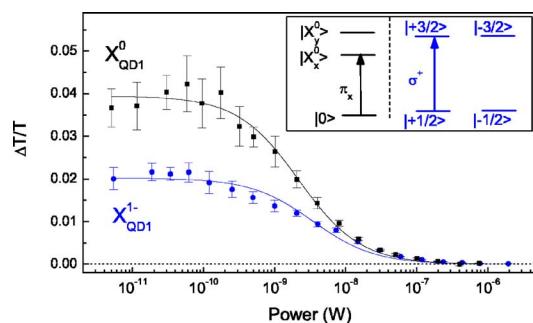


FIG. 2. (Color online) Saturation curves for the  $X^{1-}$  and  $X^0$  transitions for the same QD. The inset shows level diagrams and the polarizations used in the measurements for the two transitions. The  $X^0$  contrast is  $1.93 \pm 0.20$  times larger than the  $X^{1-}$  contrast.

measured a radiative recombination lifetime of 0.75 ns for this  $X^0$  (QD3), corresponding to a homogeneous linewidth of  $0.88 \mu\text{eV}$ . In this sample, we measure in transmission a distribution for  $\Gamma$  between 0.9 and  $4.5 \mu\text{eV}$ . The additional broadening mechanism has been attributed to temporal fluctuations in the resonance position of the QD.<sup>6</sup> The origin of such a mechanism has not yet been verified; possibilities include electrostatic fluctuations in the back contact or nearby QDs. Measurements with integration times (bandwidths) between 0.05 (3.3) and 50 s (0.003 Hz) yield the same  $\Gamma$ , suggesting that the fluctuation dynamics are on a submicrosecond time scale. Thus, access to a smaller integration time is needed to characterize the spectral fluctuation and identify ways to eliminate it. In the ideal limit, the maximum contrast below the saturation power ( $\alpha_{\text{max}}$ ) is proportional to the scattering cross section divided by the incident laser spot area ( $A$ ) and independent of the oscillator strength  $\alpha_{\text{max}} = 3(\lambda/n)^2/(2\pi A)$ , whereas the area of the absorption curve is proportional to the oscillator strength.<sup>9</sup> In a real experiment, the contrast is reduced by a geometrical factor determined by the numerical aperture of the excitation and collection optics, detector size, and distance between the detector and sample as it is impossible to collect all the light scattered by the quantum dot. We estimate that this factor is close to 2 in our experimental configuration. For  $\lambda = 950 \text{ nm}$  and  $\Delta x = 760$  (380) nm, we can expect a contrast of  $\sim 2.5$  (10.1)%, roughly three times the measured values. Assuming that the energy-integrated scattering is constant in the presence of the electrostatic fluctuations reconciles the discrepancy between the predicted and measured contrasts. Naturally, further reduction in the spot size is possible using a SIL with a larger  $n$  or of the Weierstrass geometry.

Figure 2 compares the saturation curves for  $X^0$  and  $X^{1-}$  from the same QD. The oscillator strengths are nearly equal,<sup>13</sup> yet the maximum contrast of  $X^0$  in the limit of low power is  $1.93 \pm 0.20$  times that of  $X^{1-}$ . The ground electron (hole) states in a QD are degenerate with respect to their spin projection  $\pm 1/2$  ( $\pm 3/2$ ) at zero magnetic field. Resonant excitation of a singly negatively charged QD creates a trion consisting of two electrons and a hole ( $X^{1-}$ ), for which there is zero total electron spin, and hence the electron-hole exchange interaction is turned off. However, due to the Pauli principle, the polarization of the optical excitation must excite an electron opposite in spin to the resident electron. In our devices, at the appropriate bias, an unpolarized electron tunnels into the QD from the back gate. Also, at zero magnetic field, the electron spin relaxation time is much shorter than the integration time used in the measurement, ensuring that the electron has a random spin orientation.<sup>14</sup> Hence, there is a 50% probability that the optical excitation will create the  $X^{1-}$ . Figure 2 confirms that transmission spectroscopy is sensitive to the spin of a resident electron in a QD, but the relatively long integration time measures an average of the carrier spin. If the integration time can be made smaller than the electron spin relaxation time, the contrast would switch between two discrete levels in real time due to electron spin quantum jumps.

Spectral fluctuation and carrier spin flips in the QD occur on a much faster time scale than the present integration time; therefore, a significant challenge in QD spectroscopy is to increase the detection frequency to resolve these individual events. The integration time in our experiment is de-

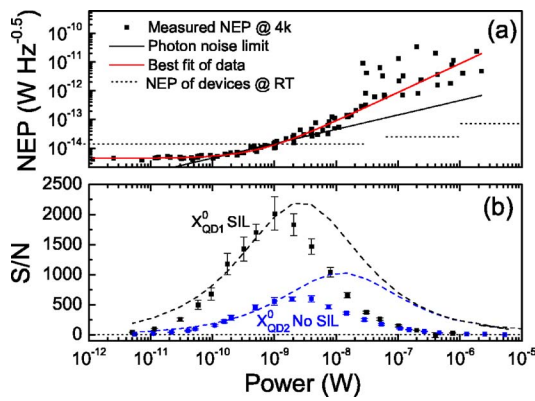


FIG. 3. (Color online) (a) NEP of our measurement system as a function of incident laser power. The straight solid line corresponds to the shot noise from the laser, the curved line is a best fit to the data, and the dashed lines are the combined room temperature NEP of the preamplifier and the detector. (b)  $S/N$  as a function of incident laser power. The signal from Fig. 1(b) and the noise from the fit in (a) are used to determine the experimental  $S/N$ . The dashed lines correspond to the ideal case when the laser shot noise dominates.

terminated by the signal to noise ratio ( $S/N$ ) of the system, where  $S$  is the differential transmission at zero detuning and  $N$  is the standard deviation of the measured transmission. The main experimental noise sources are the detector, the current preamplifier, and the shot noise of the laser light. A useful figure of merit to quantify the device noise is the noise equivalent power (NEP), which specifies the root mean square (rms) value of a sinusoidally modulated input signal that yields a rms output signal equal to the rms noise in the device. The combined room temperature NEP of the detector and current preamplifier listed by the manufacturers are 13.9, 24.7, and  $72.7 \text{ fW/Hz}^{0.5}$  at  $10^9$ ,  $10^8$ , and  $10^7$  amplifications, respectively. The shot noise from the laser is the square root of the incoming photon rate. Figure 3(a) shows the NEP as a function of power measured off-resonance from any QD transition. The measurements were performed under nominally identical conditions; however they were taken over several days and the exact environment (i.e., electrical noise, mechanical vibrations, etc.) may have changed, which accounts for the scatter in the data. The minimum NEP at a certain excitation power can be considered the ideal system performance. In the low power regime the measured NEP is  $4.5 \text{ fW/Hz}^{0.5}$ , which is likely less than the expected room temperature NEP ( $13.9 \text{ fW/Hz}^{0.5}$ ) due to a reduction in the thermal noise of the photodiode. In the high power regime the NEP increases due to the decreased current preamplifier sensitivity and the photon noise.

Figure 3(b) shows the  $S/N$  for the two QDs presented in Fig. 1(b), with and without a SIL. The noise used to determine the  $S/N$  in the plot is the best fit to the data points in Fig. 3(a) ( $\text{NEP} = \alpha + \beta P$ , where  $\alpha = 4.5 \times 10^{-15} \text{ fW/Hz}^{0.5}$  and  $\beta = 8.0 \times 10^{-6} \text{ Hz}^{-0.5}$ ), which represents the typical system noise. The dashed lines correspond to the idealized  $S/N$  with no noise from the equipment:  $S$  is calculated using the two-level model with the contrast in the low power regime from Fig. 1(b) and  $N$  is the laser shot noise. The maximum  $S/N$  when using the SIL ( $\sim 2000/\text{Hz}^{0.5}$ ) is approximately four times larger than without a SIL. In the saturation regime, the  $S/N$  does not depend on the spot area. In the low power

regime, the  $S/N$  decreases due to the decreasing signal but constant noise.

With a repetitive signal, averaging over many cycles improves the  $S/N$  in proportion to  $\eta^{0.5}$ , where  $\eta$  is the number of cycles. Based on a  $S/N$  of 2000 at 1 Hz, one can expect a signal to still be observable (i.e.,  $S/N=1$ ) at a 4 MHz bandwidth ( $\sim 0.5 \mu\text{s}$  integration time). However, for the lock-in technique the modulation frequency generally should be ten times larger than the measurement frequency. The  $RC$  time constant of our device ( $\sim 500 \text{ ns}$ ) is sufficient for megahertz frequency modulation, but the bandwidth of our preamplifier is limited to 1.2 kHz using  $10^9$  amplification. One strategy to circumvent the preamplifier bandwidth limit is perhaps to measure reflection rather than transmission.<sup>8</sup> In this case the detector can be located outside the cryostat at room temperature and an avalanche photodiode with internal gain can be used, thus reducing the required signal amplification.

In summary, we have examined how the size of the laser spot, the laser polarization, the incident laser power, and the spin state of a resident electron affect the contrast in transmission spectroscopy of a QD. By using a SIL, we have demonstrated an increase in the maximum contrast and  $S/N$  by a factor of 5 due to the reduced spot size. The increase in the  $S/N$  makes measurements in the megahertz regime possible. This capability will allow further investigation into spectral fluctuations, hopefully leading to a strategy to eliminate them. Furthermore, real time measurement of electron spin flips in semiconductor QDs may become possible, allowing direct probing of spin relaxation dynamics.

The authors acknowledge the financial support for this work from EPSRC (UK), SANDiE (EU); and DAAD and SFB631 (DE).

- <sup>1</sup>V. Cerletti, W. A. Coish, O. Gywat, and D. Loss, *Nanotechnology* **16**, R27 (2005).
- <sup>2</sup>M. Kroutvar, Y. Ducommun, D. Heiss, M. Bichler, D. Schuh, G. Abstreiter, and J. J. Finley, *Nature (London)* **432**, 81 (2004).
- <sup>3</sup>X. Q. Li, Y. W. Wu, D. Steel, D. Gammon, T. H. Stievater, D. S. Katzer, D. Park, C. Piermarocchi, and L. J. Sham, *Science* **301**, 809 (2003).
- <sup>4</sup>B. Alén, F. Bickel, K. Karrai, R. J. Warburton, and P. M. Petroff, *Appl. Phys. Lett.* **83**, 2235 (2003).
- <sup>5</sup>J. R. Guest, T. H. Stievater, X. Q. Li, J. Cheng, D. G. Steel, D. Gammon, D. S. Katzer, D. Park, C. Ell, A. Thranhardt, G. Khitrova, and H. M. Gibbs, *Phys. Rev. B* **65**, 241310 (2002).
- <sup>6</sup>A. Högele, S. Seidl, M. Kroner, K. Karrai, R. J. Warburton, B. D. Gerardot, and P. M. Petroff, *Phys. Rev. Lett.* **93**, 217401 (2004).
- <sup>7</sup>S. Seidl, M. Kroner, P. A. Dalgarno, J. M. Smith, A. Hogege, M. Ediger, B. D. Gerardot, J. M. Garcia, P. M. Petroff, K. Karrai, and R. J. Warburton, *Phys. Rev. B* **72**, 195339 (2005).
- <sup>8</sup>B. Alén, A. Högele, M. Kroner, S. Seidl, K. Karrai, R. J. Warburton, A. Badolato, G. Medeiros-Ribeiro, and P. M. Petroff, *Appl. Phys. Lett.* **89**, 123124 (2006).
- <sup>9</sup>K. Karrai and R. J. Warburton, *Superlattices Microstruct.* **33**, 311 (2003).
- <sup>10</sup>M. Atature, J. Dreiser, A. Badolato, A. Hogege, K. Karrai, and A. Imamoglu, *Science* **312**, 551 (2006).
- <sup>11</sup>M. Atature, J. Dreiser, A. Badolato, and A. Imamoglu, *Nat. Phys.* **3**, 101 (2007).
- <sup>12</sup>M. Bayer, G. Ortner, O. Stern, A. Kuther, A. A. Gorbunov, A. Forchel, P. Hawrylak, S. Fafard, K. Hinzer, T. L. Reinecke, S. N. Walck, J. P. Reithmaier, F. Klopff, and F. Schafer, *Phys. Rev. B* **65**, 195315 (2002).
- <sup>13</sup>P. A. Dalgarno, J. McFarlane, B. D. Gerardot, R. J. Warburton, K. Karrai, A. Badolato, and P. M. Petroff, *Appl. Phys. Lett.* **89**, 043107 (2006).
- <sup>14</sup>P. F. Braun, X. Marie, L. Lombez, B. Urbaszek, T. Amand, P. Renucci, V. K. Kalevich, K. V. Kavokin, O. Krebs, P. Voisin, and Y. Masumoto, *Phys. Rev. Lett.* **94**, 116601 (2005).